



ISSN: 2329-8200 (Print)
ISSN: 2329-8197 (Online)

CODEN : JBSOC4

Journal of Biopharmaceutics Sciences (JBS)

DOI : <http://doi.org/10.26480/jbs.01.2017.10.13>



EXPERIMENTAL STUDY ON THE CIRCUMFERENTIAL RESIDUAL STRAINS IN AORTIC ARCH BASED ON CURVE LENGTH METHOD

Zhang Xiaojun*, Li Xiaoyang

School of Mechanical Engineering and Applied Electronics Technology, Beijing University of Technology, Beijing 100124, China

*Corresponding Author's E-mail: xjzhang@bjut.edu.cn

This is an open access article distributed under the Creative Commons Attribution License, which permits unrestricted use, distribution, and reproduction in any medium, provided the original work is properly cited

ARTICLE DETAILS

Article History:

Received 7 January 2017
Accepted 10 February 2017
Available online 15 February 2017

ABSTRACT

In order to quantify residual strains in aortic arch, curve length method and corresponding computerized measurement of vessel images are presented. Distributions of geometric parameters and circumferential residual strains in rabbit aortic arch have been investigated. Subsequently, circumferential residual strains of aortic arch in the zero-stress state were calculated. As results of the experiment and calculation, axial distribution of residual strains in inner or outer walls along aortic arch is consistent well with the opening angle distribution, in which the variation magnitude is much smaller in the straight section than in the curved section. Simultaneously, not only the opening angle but also residual strains aren't the function of circumferential coordinate θ , which means that circumferential distributions of the opening angle and residual strains are uniform. Furthermore, radial distribution of circumferential residual strains is nonlinear, and the radial gradient minimizes at the arch of aorta approximately.

KEYWORDS

Aortic Arch, Residual Strains, Zero-stress State, Curve Length Method

1. INTRODUCTION

Based on a study, it has been known since 1960 that when a ring segment is cut from an aortic and a radial cut is made in the ring, it uncoils like a watch spring, but this phenomenon wasn't explained with residual strains and stresses in blood vessel until 1983 [1-3]. They suggested that residual stress developed in growing arteries so as to reduce stress gradients across the wall thickness. Another illustration, which termed the uniform strain hypothesis, was adopted by a researchers who assumed that, under physiological conditions, the circumferential strains are constant across the thickness of a blood vessel wall [4]. Foundation of residual strains has not only changed traditional analytic methods of strains and stresses in blood vessel, but also confirmed the existence of dynamics situations in cell growth and self-optimization in organism. Furthermore, the zero-stress state provided the exact initial situations for strains and stresses analyzation of blood vessel. Studies on the vascular residual strains have become one of the most attractive subjects of biomechanics in last 20 years [5].

However, studies on curved and bifurcate vessel are limited in theoretic modeling. For example, a researcher presented a theoretical model to analyze the non-linear elastic properties of the aortic arch wall [6]. Fortunately, computerized measurements of images have developed to carry out experimental study on residual strains in curved aorta recently.

2. CURVE LENGTH METHOD OF RESIDUAL STRAINS

According to a researcher, the curve length method is based on computerized measurements in which the inner curve length C_i , the outer curve length C_o , and the mean thickness h of the ring segment in the zero-stress state are measured [7]. Consequently, a standard circle can be derived from the non-uniform ring segment according to C_i , C_o and h .

Corresponding transformation equation is defined as

$$\varphi_o = \frac{C_o - C_i}{h}, r_i^* = \frac{C_i}{\varphi_o}, r_o^* = r_i^* + h \quad (1)$$

Where, C_o —inner curve length of aortic wall in zero-stress state (m ; C_i —outer curve length of aortic wall in zero-stress state (mm) ; h —mean thickness of aortic wall in zero-stress state (mm) ; r —inner radius of standard circle(mm) ; r^* —outer radius of standard circle(mm) ; φ_0 —radius angle of standard circle , $\varphi_0=2\alpha(^{\circ})$; α —semi radius angle of standard circle, or opening angle($^{\circ}$) .

In curve length method, the blood vessel was assumed as uniform anisotropic incompressible materials. Thus, the Cauchy-Green stress is

$$E_i = \frac{1}{2}(\lambda_i^2 - 1) \quad (2)$$

Where, index i refers to the axial direction z , circumference direction θ and radial direction r , respectively, and λ_i is the stretch ratio. For instance, the circumferential stretch ratio is

$$\lambda_{\theta} = \frac{\pi r}{\alpha r^*} \quad (3)$$

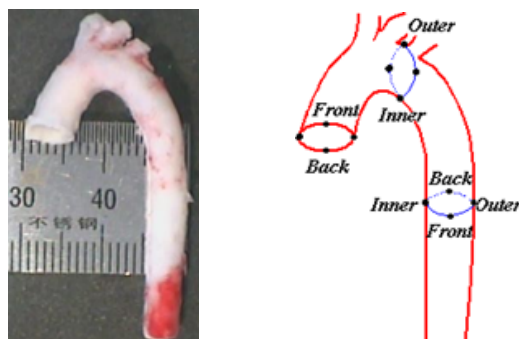
Where r^* is the radius of standard circle arterial segment in zero-stress state, and r is the radius of arterial segment in non-loaded state, which can be calculated according to the incompressibility.

$$r^2 = r_o^2 - \frac{\theta_o}{\pi \lambda_z} (r_o^{*2} - r_i^{*2}) \quad (4)$$

Where r_o is the outer radius of blood vessel in the non-loaded state, r is the outer radius of blood vessel in the zero-stress state, and λ_z is the stretch ratio in axial direction of blood vessel in the non-loaded state. Consequently, circumferential residual strains can be calculated, only if the parameters C_o , C_i , h and r_o are measured in the experiment -loaded state, which can be calculated according to the incompressibility.

3. MATERIALS AND MEASUREMENTS

Four 4-5 months old healthy purebred rabbits are chosen in the experiment. And the experiment was conducted within the animal welfare regulations and guidelines of China. Surgery was performed under intravenous celiac pentobarbital anesthesia (30mg/kg), and aortic arch in the non-loaded state was dissected from each rabbit, which was recorded (Figure 1a) in the computer via a CCD camera (WV-CL700, Panasonic, Osaka, Japan). As seen in Figure 1b, in order to investigate different radial cutting directions, four representative directions were marked, which were labeled as Inner, Outer, Front and Back



(a) The experimental rabbit sample (b) Four cut-open directions

Figure 1: The aortic arch

About 1mm-long ring specimens in the non-loaded state were obtained after axial cutting along each rabbit aortic arch, independently, and were recorded in the computer via CCD camera after immersed in saline solution at room temperature. Then, the segments, floating in saline solution, were cut along the radial direction in the sequence of Outer, Back, Inner and Front. And configurations of transverse cross sections were again recorded in computer after about twenty minutes. Elliptic curve fitness and parabola fitness, which combine computerized measurements of images, are applied to measure the curve length of aortic wall in the non-loaded state and in the zero-stress state separately.

4. EXPERIMENTAL RESULTS

In the experiment, cross-sectional configuration parameters of aortic arch, such as semi-major/semi-minor axis, mean wall thickness of the arterial wall in the non-loaded state, and inner/outer curve length, mean wall thickness of the arterial wall in the zero stress state, were measured. Furthermore, according to curve length method, the opening angle distribution and circumferential residual strain distribution in aortic arch were calculated using measured geometric parameters.

4.1 Geometric parameters of aortic arch in the non-loaded state

In the non-loaded state, the cross-sectional boundary line of aortic ring was fitted with elliptic curve. And statistic results of the semi-major and semi-minor axis of the fitted ellipse are given in Table 1.

Table 1: Results in the non-loaded state

	05108 N=29		05115 N=38		05123 N=32		05129 N=47	
	<u>Mean</u>	<u>S.D.</u>	<u>Mean</u>	<u>S.D.</u>	<u>Mean</u>	<u>S.D.</u>	<u>Mean</u>	<u>S.D.</u>
a_i	2.158	0.178	2.286	0.303	2.158	0.178	2.286	0.303
b_i	1.711	0.185	1.697	0.232	1.711	0.185	1.697	0.232
a_e	2.507	0.199	2.689	0.328	2.507	0.199	2.689	0.328
b_e	<u>2.097</u>	<u>0.192</u>	<u>2.133</u>	<u>0.265</u>	<u>2.097</u>	<u>0.192</u>	<u>2.133</u>	<u>0.265</u>
e_i	0.796	0.092	0.747	0.091	0.796	0.092	0.747	0.091
e_e	<u>0.839</u>	<u>0.078</u>	<u>0.796</u>	<u>0.078</u>	<u>0.839</u>	<u>0.078</u>	<u>0.796</u>	<u>0.078</u>
T_o	0.349	0.060	0.384	0.070	0.349	0.060	0.384	0.070
T_i	0.352	0.065	0.407	0.053	0.352	0.065	0.407	0.053
T_f	0.385	0.060	0.433	0.075	0.385	0.060	0.433	0.075
T_b	<u>0.388</u>	<u>0.061</u>	<u>0.408</u>	<u>0.069</u>	<u>0.388</u>	<u>0.061</u>	<u>0.408</u>	<u>0.069</u>
$E_{\theta i}$	-0.032	0.028	-0.040	0.027	-0.031	0.036	-0.018	0.026
$E_{\theta e}$	0.009	0.011	0.018	0.036	0.012	0.036	0.013	0.028

Where, a_i , b_i -semi-major and semi-minor axis of inner fitness ellipse respectively(mm); a_e , b_e -semi-major and semi-minor axis of outer fitness ellipse respectively(mm); e_i , e_e -ellipticity of inner wall and outer wall separately; T_o , T_i , T_f , T_b -thickness in outer, inner, Front and Back directions separately(mm); $E_{\theta i}$, $E_{\theta e}$ -residual strains in inner and outer wall separately.

4.2 Geometric parameters of aortic arch in the zero-stress state

Corresponding to elliptic curve fitness in the non-loaded state, parabola fitness was explored in the zero-stress state. In detail, the curve length measurement is three-point-parabola fitness aiming at different subsections of the whole wall curve. And corresponding statistic results of inner and outer curve length are given in Table 2. Furthermore, Table 2 shows statistic wall thicknesses in four positions of aortic wall in the zero-stress state.

Table 2: Results in the zero-stress state

	<u>05108 N=29</u>		<u>05115 N=38</u>		<u>05123 N=32</u>		<u>05129 N=47</u>	
	<u>Mean</u>	<u>S.D.</u>	<u>Mean</u>	<u>S.D.</u>	<u>Mean</u>	<u>S.D.</u>	<u>Mean</u>	<u>S.D.</u>
C_e	14.34	1.039	14.87	1.405	14.34	1.039	14.87	1.405
C_i	<u>12.59</u>	<u>1.052</u>	<u>13.05</u>	<u>1.516</u>	<u>12.59</u>	<u>1.025</u>	<u>13.05</u>	<u>1.516</u>
T_o	0.417	0.078	0.568	0.089	0.417	0.078	0.568	0.089
T_i	0.434	0.080	0.586	0.097	0.434	0.080	0.586	0.097
T_f	0.434	0.074	0.601	0.089	0.434	0.074	0.600	0.089
T_b	<u>0.394</u>	<u>0.057</u>	<u>0.533</u>	<u>0.078</u>	<u>0.394</u>	<u>0.057</u>	<u>0.533</u>	<u>0.078</u>
α	58.99	25.81	88.69	22.88	88.92	41.51	49.75	37.08

Where, C_e , C_i -the length of inner and outer curve respectively (mm); T_o , T_i , T_f , T_b -thickness in outer, inner, Front and Back directions separately(mm); α -the opening angle ($^{\circ}$).

According to curve length method, the opening angle and circumferential residual strain can be computed through equations (1)-(4), in which all required parameters have been measured. The results are presented in Table 1 and Table 2.

As shown in Table 1, circumferential residual strains in inner aortic wall are negative, which means that the inner aortic wall is compressible. On the contrary, circumferential residual strain in outer aortic wall is positive, so the outer aortic wall is tensile. In the pig's and cow's experiments, a researcher also found that residual strains are negative at the inner part and are positive at the outer part of arterial wall, with which the present rabbit's results are consistent well [2].

5. DISCUSSIONS

5.1 Distribution of geometric parameters in non-loaded state

The cross-sectional configuration of aortic ring in the non-loaded state should be circle ideally. However, the aortic ring configuration was found to be elliptic in the experiment. Thus, the cross-sectional ellipticity was defined by

$$e = b / a \quad (5)$$

And the ellipticity, which can be seen in Table 1, was calculated according to measured semi-major axis and semi-minor axis. It is concluded that the cross-sectional configuration is elliptic in curved aortic section but is circle nearly in straight section.

5.2 Distribution of aortic wall thickness

Firstly, circumferential distribution of the aortic wall thickness was investigated. Comparing the wall thicknesses in four representative positions in Table 1, there is nearly no difference in statistic. Therefore, the wall thickness of aortic arch in the non-loaded state is uniform in circumferential direction. And the same conclusion can be drawn in the zero-stress state according to Table 2. The results show that the amplitude of variation in aortic wall thickness, not only in the non-loaded state, but also in the zero-stress state, is big in the curved section but is small in the straight section separately.

5.3 Axial distribution of the opening angle and residual strains

a group of researchers have reported that the opening angle varies with location in the aortic tree, which has been ascribed to non-uniform wall structure [8,9]. Figure 2 shows the axial distributions of the opening angle in the zero-stress state and residual strains in inner and outer walls in the non-loaded state. And it is concluded that the amplitudes of variation, not only for the opening angle but also for residual strains, are much smaller in the straight section than in the curved section. Especially, residual strains in the straight section of aortic arch can be assumed as a constant. Furthermore, the relation between the opening angle and residual strains is positive correlativity.

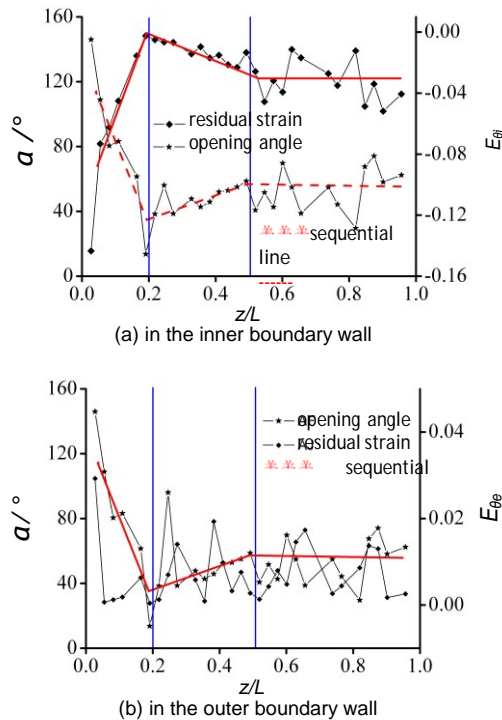
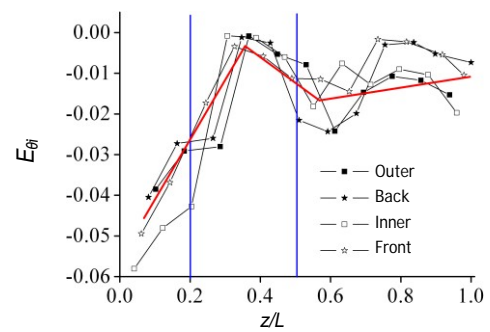
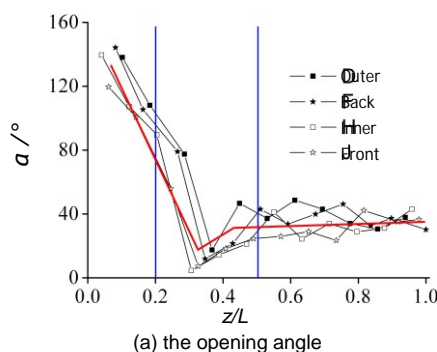


Figure 2: Axial distribution of averaged thickness

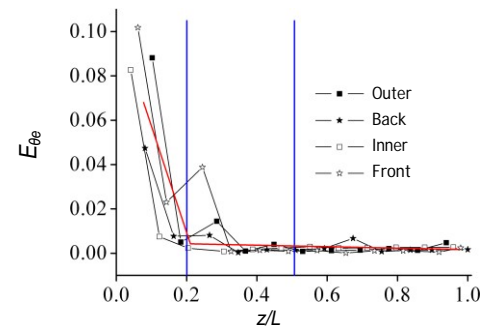
5.4 Circumferential distribution of the opening angle and residual strains

As seen in Figure 3, experimental results are counted according to four representative circumferential positions separately. And statistical comparison indicates that the four representative circumferential distributions nearly have the same sequential line. Thus it is concluded that not only the opening angle but also residual strains aren't the function of circumferential coordinate θ .

On the other hand, the experiment was carried out on the assumption that deformation field in the zero-stress state should be non-uniform only if the circumferential distribution of residual strains in the non-loaded state is non-uniform too. Consequently, uniform deformation field measured in the experiment implies that residual strains are distributed uniformly in circumferential direction, which is coordinate with the assumption used in theoretical research about the non-linear elastic properties of aortic wall [6].



(b) residual strain in internal wall



(c) residual strain in external wall

Figure 3: Axial distribution of the physical quantities in four circumferential positions

5.5 Radial distribution of the residual strains

In order to investigate the radial distributions of residual strains, six points with 1mm spacing were chosen from inner aortic boundary wall to outer aortic boundary wall in the experiment. Subsequently, the corresponding residual strains were counted along the radial direction. Especially, representative sections of aortic arch, such as the curved section of ascending aorta, the curved section of descending aorta and the straight section of descending aorta were reviewed.

Fig. 4 presents the radial distributions of residual strains in representative sections of aortic arch. Based on a study, it was concluded that the relationship between residual strains in the three representative sections and the non-dimensional radial coordinates is nonlinear, which agrees with the stress-strain relation [10].

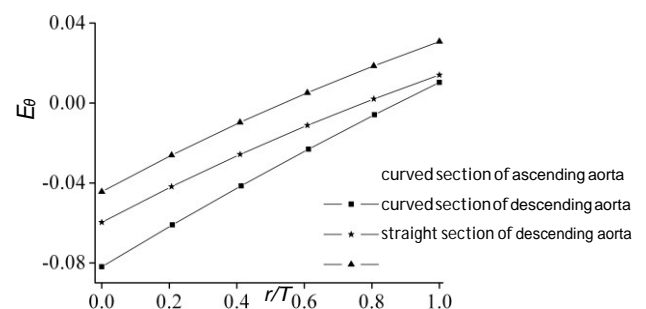


Figure 4: Radial distributions of residual strains in representative sections of aortic arch

Furthermore, the residual strain gradient in radial coordinates was defined by

$$k = \frac{E_{\theta e} - E_{\theta i}}{r_e - r_i} \quad (6)$$

As shown in Fig. 5, axial distribution of the residual strain gradient in radial coordinates indicates that the residual strain gradient takes its minimum at the arch, and the amplitude is nearly constant in the straight section of aortic arch

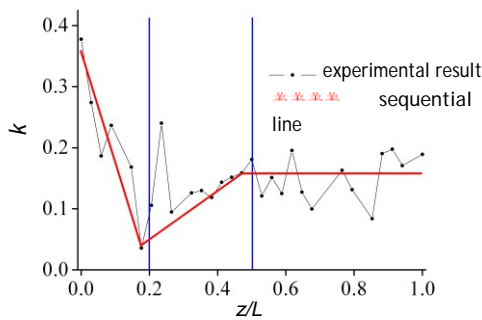


Figure 5: Axial distribution of the radial gradient of circumferential residual strains

6. CONCLUSIONS

The axial distribution of configuration parameters indicates that aortic arch in the non-loaded state is elliptic cross-section in its curved section but is circular cross-section in its straight section. Furthermore, the whole aortic arch is cone-shaped in axial direction, which agrees well with the physiologic practice. Simultaneously, circumferential distribution of averaged thickness is nearly uniform, not only in the non-loaded state but also in the zero-stress state. However, axial distribution of averaged thickness is not uniform any longer.

The results obtained in the present study also indicate that the opening angle and residual strains depend upon the location of aortic arch because of the non-uniform wall thickness in a certain extent. In detail, the opening angle is small in the straight section and is big in the curved section of aortic arch. And the magnitudes of variation are much smaller in the straight section than in the curved section. On the other hand, it is concluded that the relation between the opening angle and residual strains is positive correlativity. The dependence of the opening angle and circumferential residual strains on axial location may reflect differences in the histological structure and wall dimensions in different sections of aortic arch.

Simultaneously, not only the opening angle but also residual strains aren't the function of circumferential coordinate θ , which means that circumferential distributions of the opening angle and residual strains are uniform. Furthermore, radial distribution of circumferential residual strains presents the nonlinear property in the change experience from inner negative strain to outer positive strain. Especially, the radial gradient minimizes at the arch of aorta approximately.

ACKNOWLEDGEMENT

This work was financed by the research fund of National Natural Scientific Foundation of China (Grant No: 10372010) and Beijing Natural Scientific Foundation (Grant No: 3102008).

REFERENCES

- [1] Bergel, D.H. 1960. The viscoelastic properties of the arterial wall. PhD., University of London.
- [2] Vaishnav, R.N., Vossoughi, J. 1983. Estimation of residual strains in aortic segments, *Biomedical Engineering II, Recent Developments*, (2), 330-333.
- [3] Chuong, C.J., Fung, Y.C. 1983. Three-dimensional stress distribution in arteries, *Journal of Biomechanical Engineering*, 105, 268-274.
- [4] Takamizawa, K., Hayashi, K. 1987. Strain energy density function and uniform strain hypothesis for arterial mechanics, *Journal of Biomechanics*, 20: 7-17.
- [5] Rachev, A., Greenwald, S.E. 2003. Residual strains in conduit arteries, *Journal of Biomechanics*, 36: 661-670.
- [6] Li, X., Wu, S., Qiao, A. 1999. Theoretical analysis on the non-linear elastic properties of the aortic arch wall. *Acta Mechanica Sinica*, 31: 193-202.
- [7] Li, X., Zeng, Y. 2002. An alternative method of strain analysis on arterial walls, *Journal of Biomedical Engineering*, 19, 166-171.

[8] Fung, Y.C., Liu, S.Q. 1989. Change of residual strains in arteries due to hypertrophy caused by aortic constriction, *Circulation Research*, 65: 1340-1349.

[9] Hayashi, K., Takahama, K., Miyazaki, H. 1995. Residual strains and opening angles in aortic walls of the rabbit, In *Proceedings of the 4th China-Japan-USA-Singapore Conference on Biomechanics*. International Academic Publisher, Beijing.

[10] Liu, S.Q., Fung, Y.C. 1988. Zero-stress state of arteries, *Journal of Biomechanical Engineering*, 110: 82-84.

